Interspecies D/Ar separation in an ICF implosion inferred from imaging x-ray spectroscopy

Scott Hsu for the IonSepMMI campaign team:

Tirtha Joshi, Peter Hakel, Mark Schmitt, Nels Hoffman, Erik Vold, Rick Rauenzahn, Xianzhu Tang, Grigory Kagan, Roberto Mancini, Yongho Kim, and Hans Herrmann

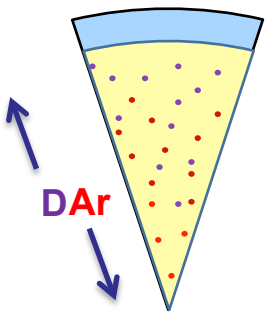

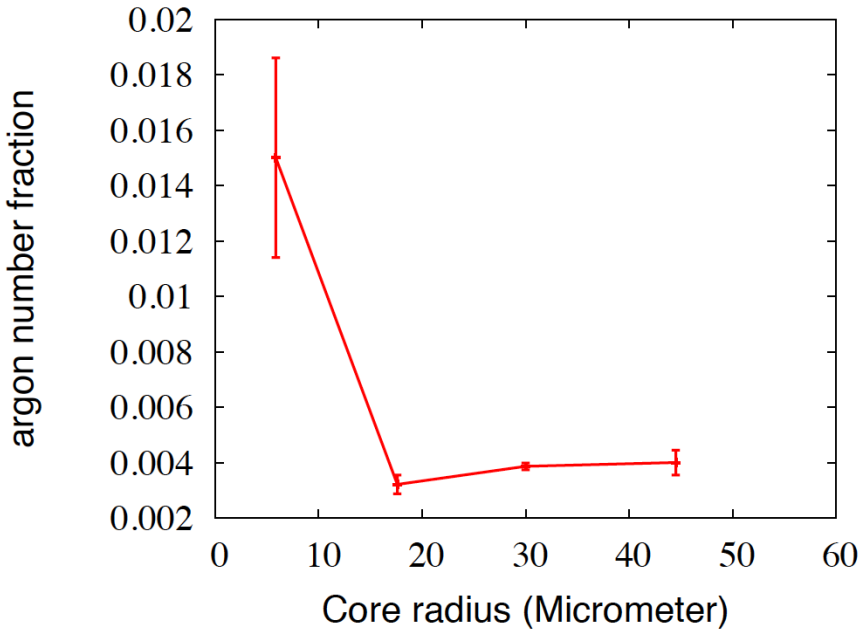

LLNL Kinetic Physics Workshop

April 5–7, 2016

Livermore, CA

Sponsored by the LANL ICF and ASC Programs.

Los Alamos NATIONAL LABORATORY EST. 1943

NNSA National Nuclear Security Administration

Talk synopsis

Concept: Strong ion thermo-diffusion between D/Ar observed via Ar K-shell spectroscopy

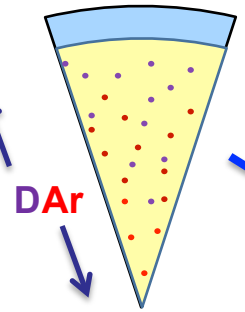

60-beam symmetric direct drive

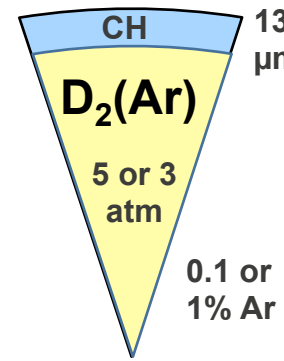

First-principles interspecies-ion-diffusion theory

$$\mathbf{i} = -\rho D\left(\nabla c + k_p \nabla \log p_i + \frac{e k_E}{T_i}\nabla\Phi + k_T^{(i)}\nabla \log T_i + k_T^{(e)}\nabla \log T_e\right)$$

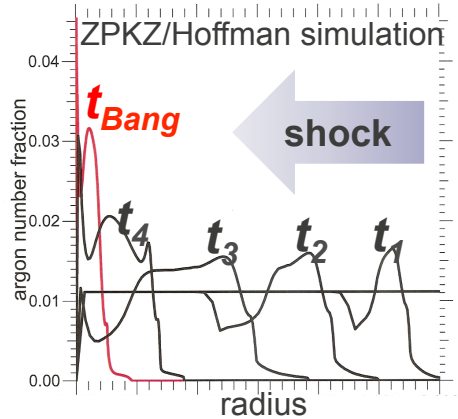

Ar enhancement/depletion around incoming shock, dominated by ion thermo-diffusion.

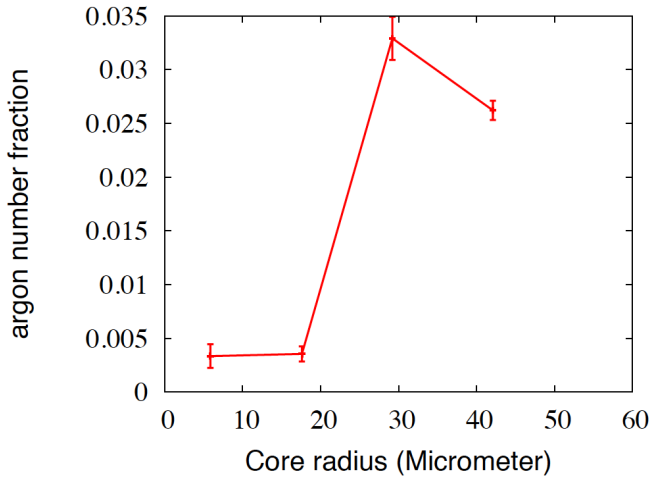

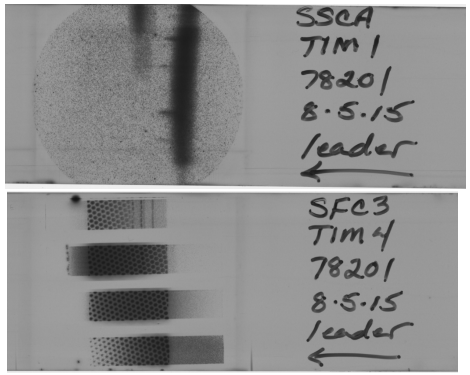

Ar H- and He-like lines

Detailed analysis including atomic/opacity modeling

Multi-fluid plasma theory of binary interspecies ion diffusion motivated and guided our campaign design

Diffusive light-ion mass flux:

$$\mathbf{i} = -\rho D\Big(\underbrace{\nabla c}_{\text{concentration}} + \underbrace{k_p \nabla \log p_i}_{\text{baro}} + \underbrace{\frac{e k_E}{T_i}\nabla\Phi}_{\text{electro}} + \underbrace{k_T^{(i)} \nabla \log T_i}_{\text{ion-thermal}} + \underbrace{k_T^{(e)} \nabla \log T_e}_{\text{electron-thermal}}\Big)$$

- Exploit ion thermo-diffusion
- Large mass difference between ion species
- Ar-doped D implosions with strong T_i gradient
- High T_i to increase D and grad T_i, but not too high such that implosion would be overly kinetic

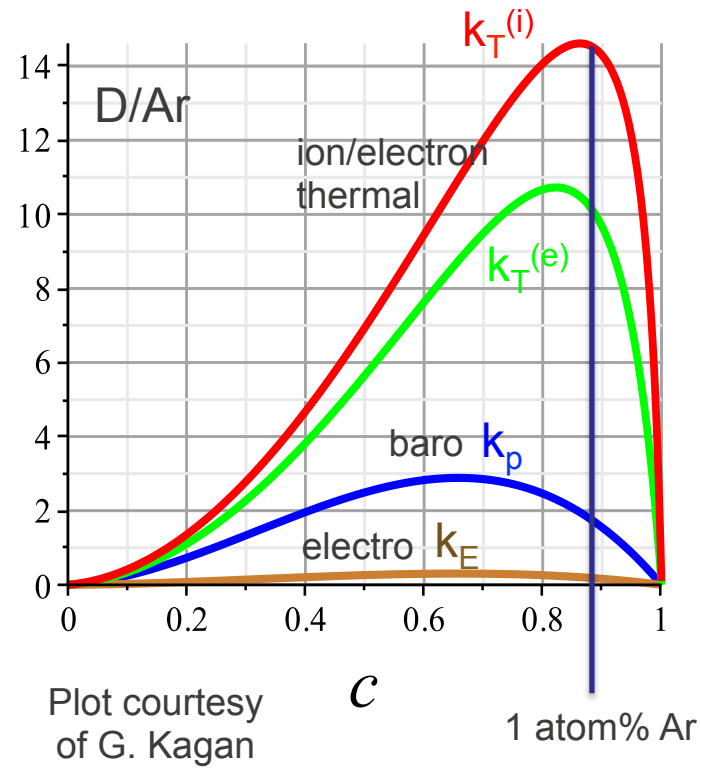

Plot courtesy of G. Kagan

G. Kagan and X.-Z. Tang, Phys. Plasmas **19**, 082709 (2012) & Phys. Lett. A **378**, 1531 (2014).

Experimental and diagnostic configurations (60-beam, symmetric direct drive on OMEGA)

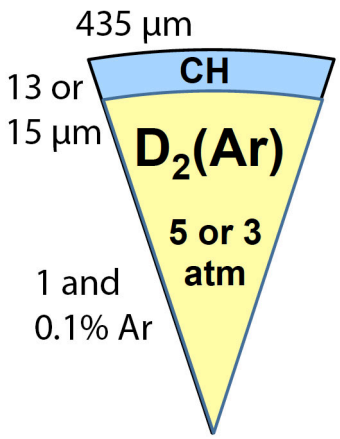

Nominal target and laser values

target type	capsule OD (μm)	shell thickness (μm)	D_2/Ar pressure (atm)	Ar atom%	laser energy (kJ)
A	870	13	5	1.0	21.5
B	870	13	5	0.1	21.5
C	870	15	3	1.0	26.0
D	870	15	3	0.1	26.0

1-ns square pulse (SG1018); SG5 phase plates

Diagnostic setup

TIM	Diagnostic	Port	Notes
1	SSCA	P3	2.9–4.3 keV, 2-ns sweep, film
2	XRS2	H3	2.84–5.0 keV, image plate
3	XRFC1/MMI	H18	3.3–5.5 keV, 10-μm pinholes, film
4	SFC3/MMI	P6	3.3–5.5 keV, 10-μm-pinholes, film
5	Large Format Camera	H14	film
6	NTOF84 (Clear_LOS)	P7	

We had 12 target shots on Aug. 5, 2015:
3 type A
3 type B
4 type C
2 type D

Key fixed diagnostics included: NTD, NTOFs, FABS, XRPHCs, GMXI, KB microscope, visible cameras.

For 1% Ar capsules, we successfully obtained SSCA/ MMI data with Ar H- and He-like K-shell line emission

15 μm/3 atm/1% Ar

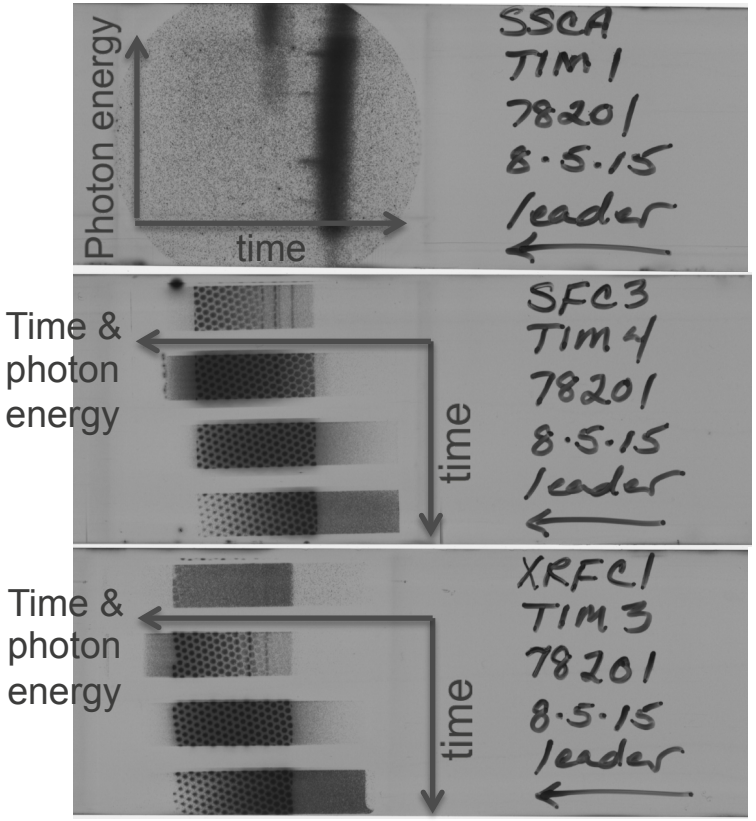

13 μm/5 atm/1% Ar

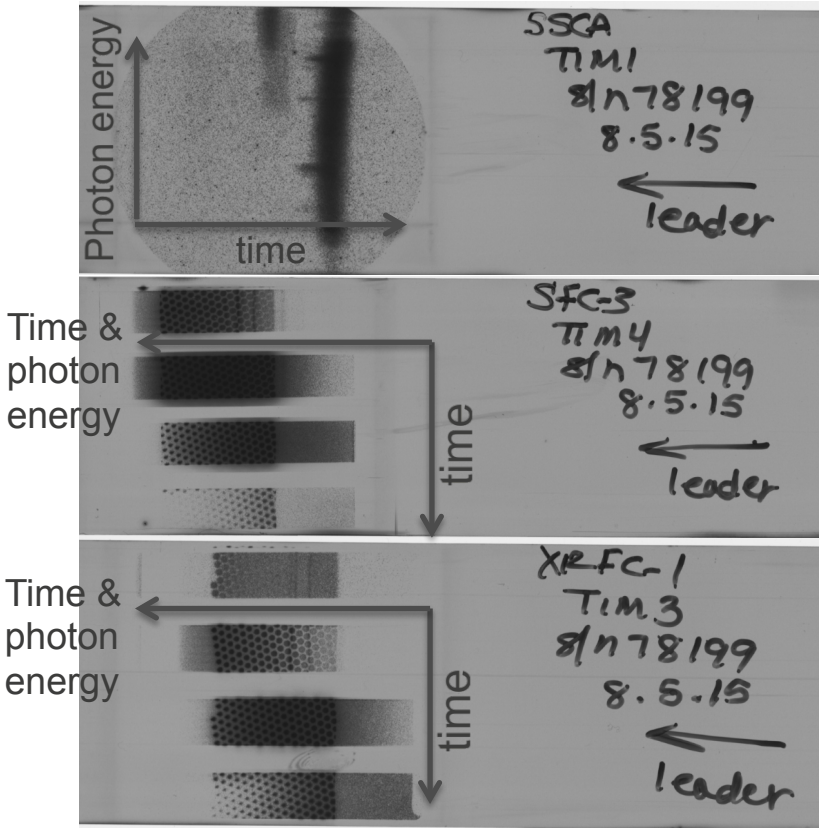

For 0.1% Ar capsules, Ar H- and He-like K-shell line emission was weaker and difficult/impossible to analyze.

We have used two different interspecies-ion-diffusion simulation models to support this campaign

Interspecies diffusion model	Approximations/ assumptions	Use
Molvig, Simakov, Vold (MSV)[1]	Binary mixture, $m_h >> m_l$	Pre- and post-shot simulations for quantitatively assessing amounts, timings, and positions of Ar-concentration enhancement and depletion
Zimmerman, Paquette, Kagan Zhdanov (ZPKZ)[2]	N species, single T_i	Post-shot simulations for quantitatively assessing amounts, timings, and positions of Ar-concentration enhancement and depletion

[1]K. Molvig, A. N. Simakov, and E. L. Vold, Phys. Plasmas **21**, 092709 (2014); [2]Kagan & Tang, Phys. Lett. A 378, 1531 (2014); C. Paquette et al., Ap. J. Suppl. Ser. **61**, 177 (1986); V. M. Zhdanov, *Transport Processes in Multicomponent Plasma*, (Taylor and Francis, New York, 2002); R. Schunk, *Rev. Geophys. Space Phys.* **15**, 429 (1977); N. Hoffman, G. Zimmerman et al., *Phys. Plasmas* **22**, 052707 (2015).

Simulations using multi-species ion-transport models show Ar depletion ahead of incoming shock followed by enhancement behind the rebounding shock

Simulated Ar atom% vs. radius at different times (ns)

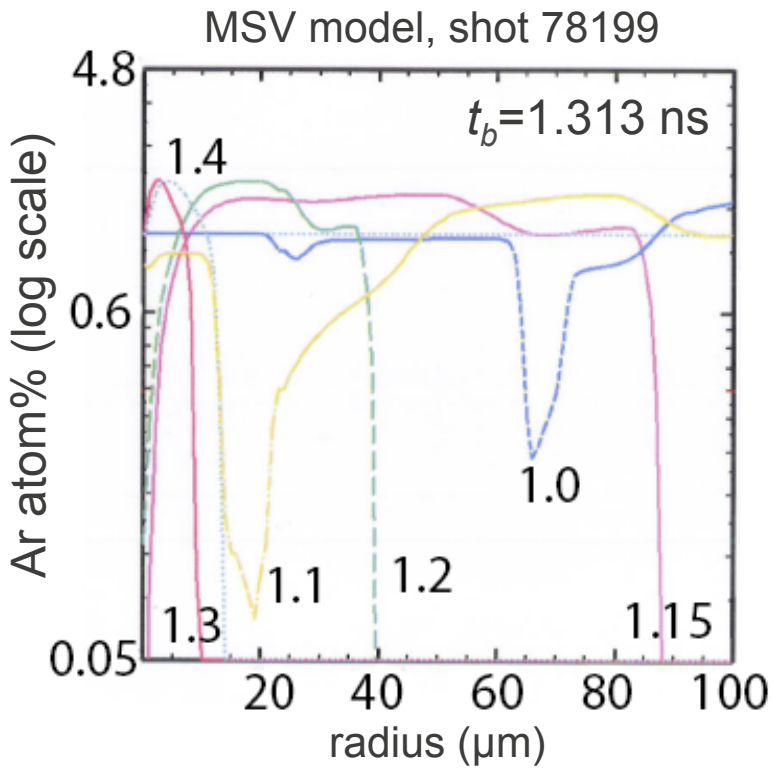

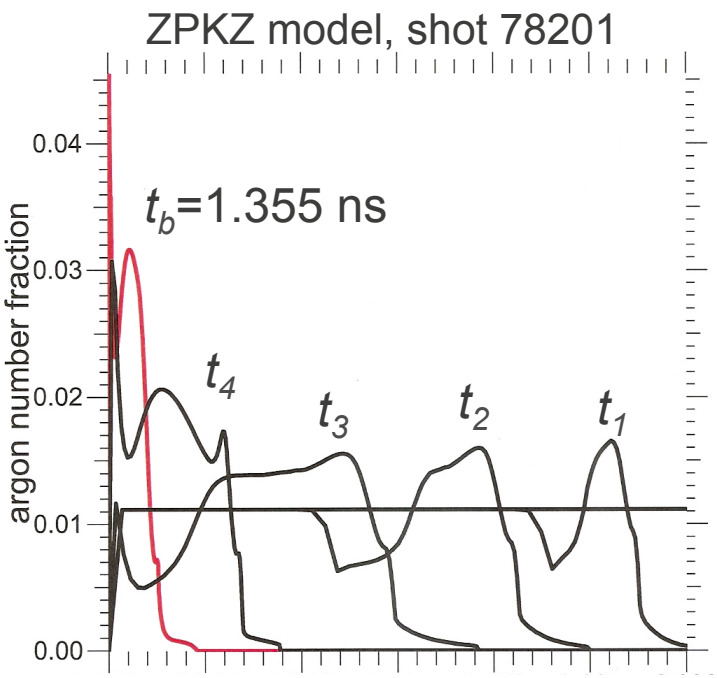

In both cases, simulations with ion thermo-diffusion turned off show no significant Ar-concentration variations from the 1% uniform pre-fill.

Ar-concentration profiles are extracted from MMI data analysis, indicating D/Ar species separation

Processed MMI data

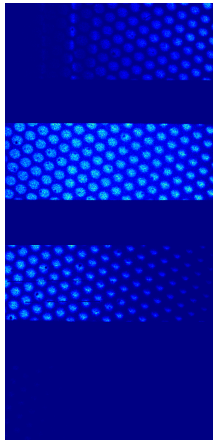

Frame 1, t=1.10 ns

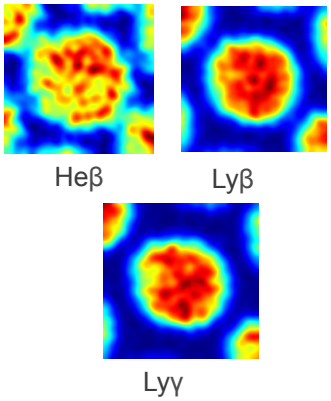

Shot 78199, XRFC1/TIM4/f1, 13 μm/5 atm/1% Ar
t_{BT}=1.313 ns, DDn=1.35E11, 21.1 kJ UV

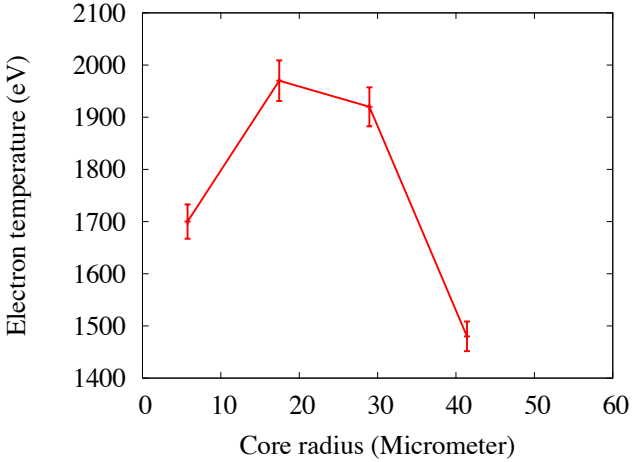

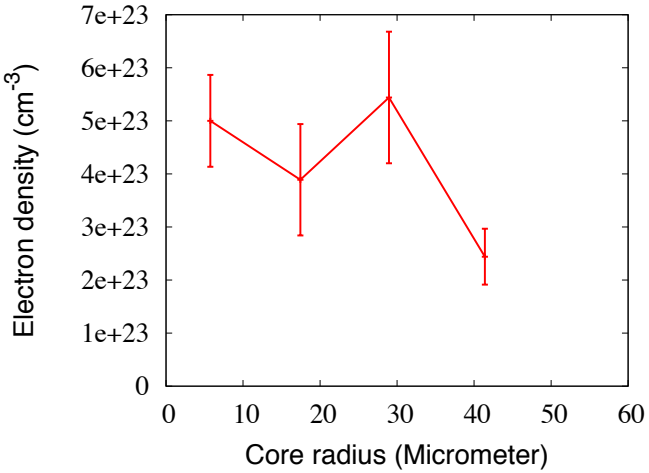

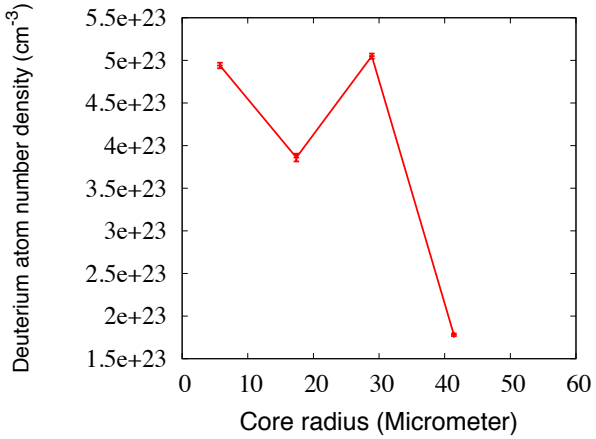

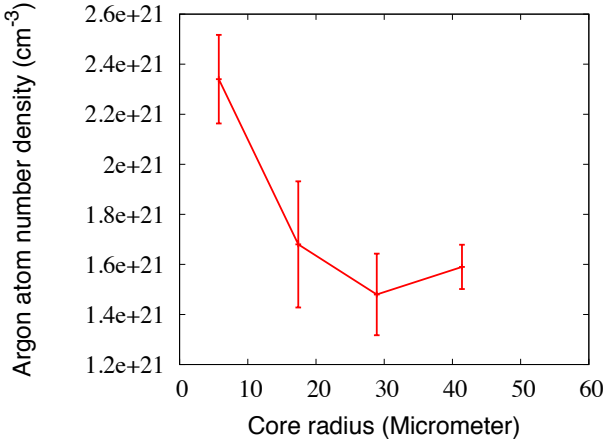

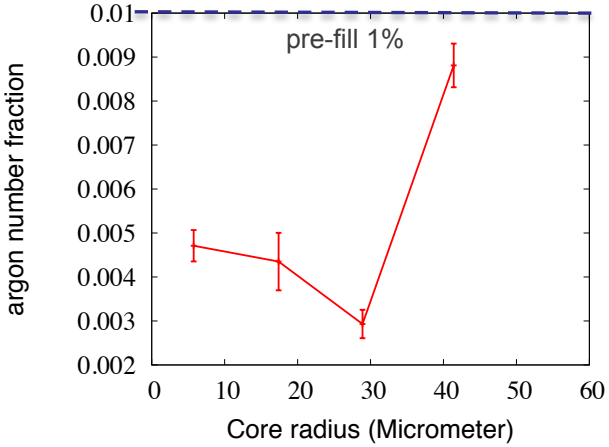

Ar-concentration profiles are extracted from MMI data analysis, indicating D/Ar species separation

Processed MMI data

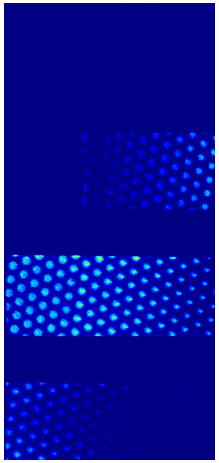

Frame 2, t=1.14 ns

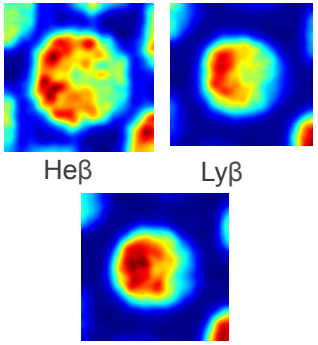

Shot 78199, XRFC1/TIM3/f2, 13 μm/5 atm/1% Ar
t_{BT}=1.313 ns, DDn=1.35E11, 21.1 kJ UV

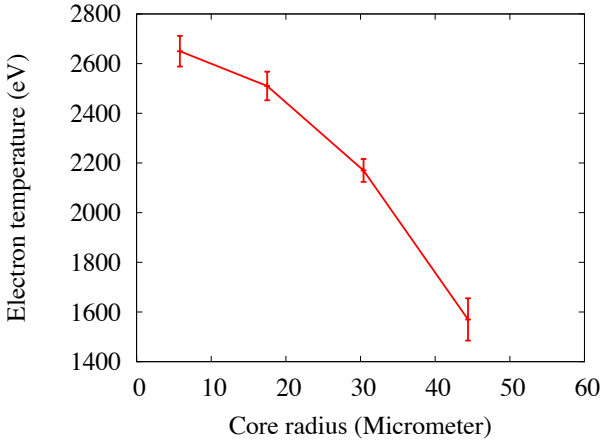

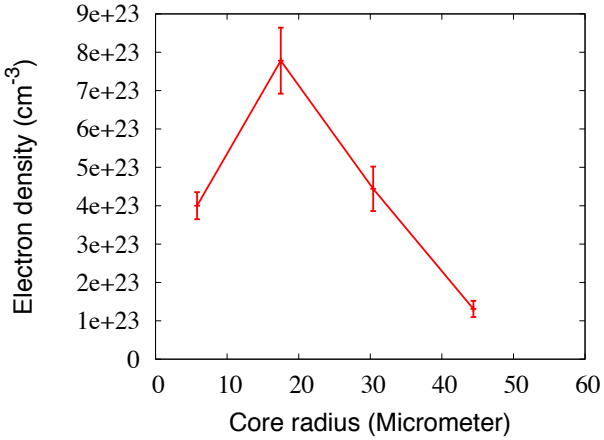

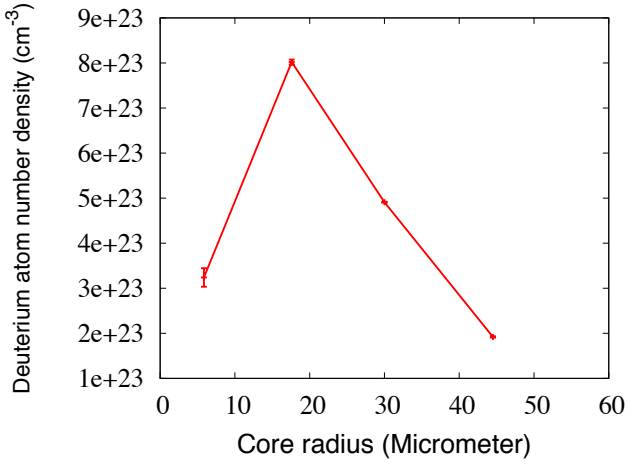

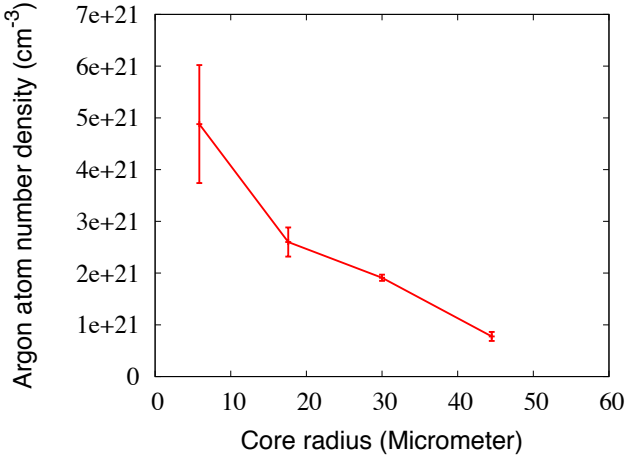

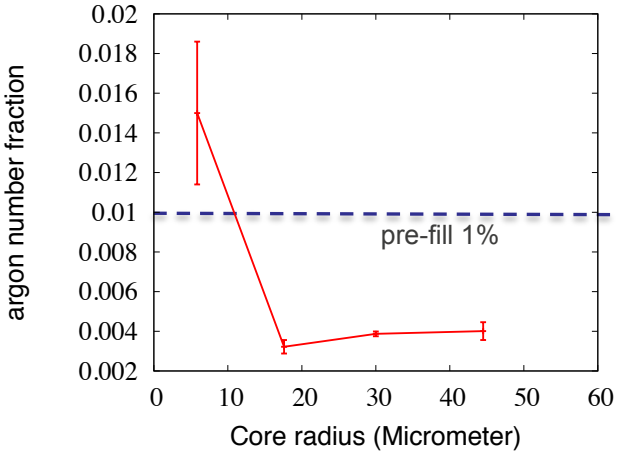

Ar-concentration profiles are extracted from MMI data analysis, indicating D/Ar species separation

Processed MMI data

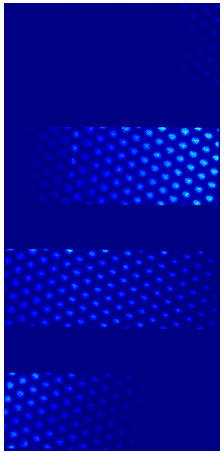

Frame 2, t=1.18 ns

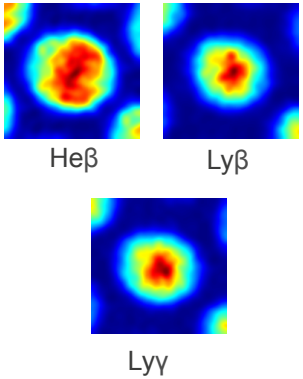

Shot 78201, SFC3/TIM4/f2, 15 μm/3 atm/1% Ar
t_{BT}=1.355 ns, DDn=8.06E10, 26.2 kJ UV

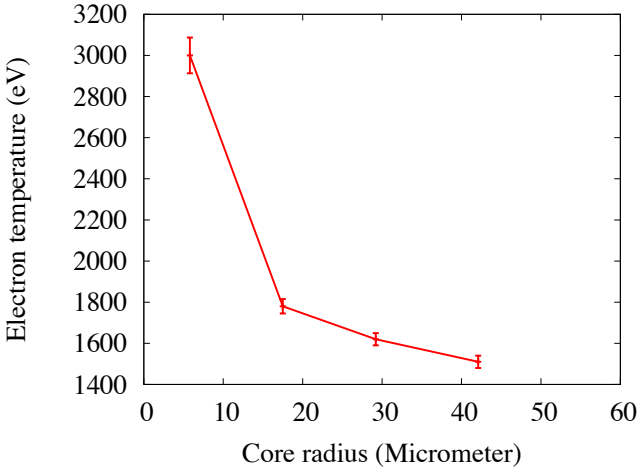

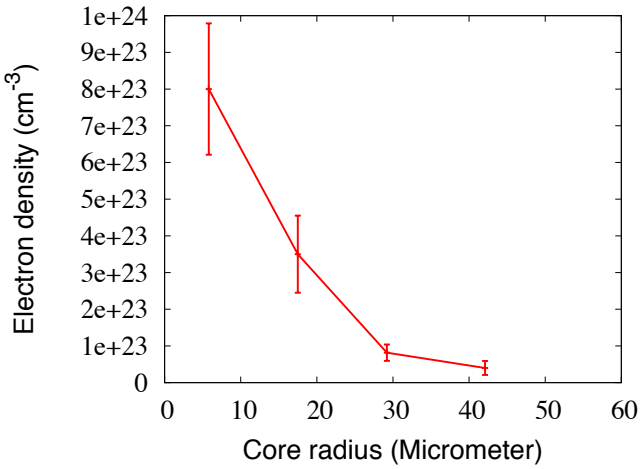

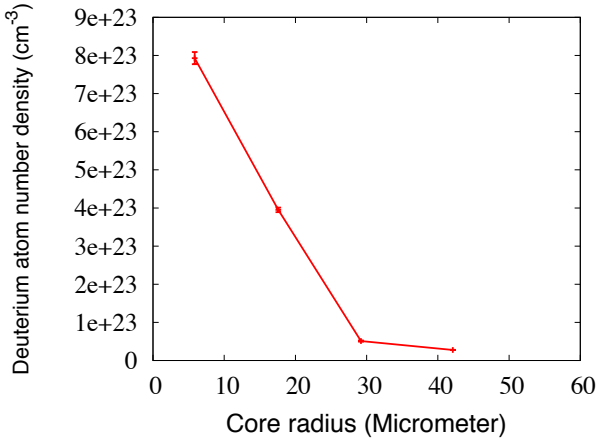

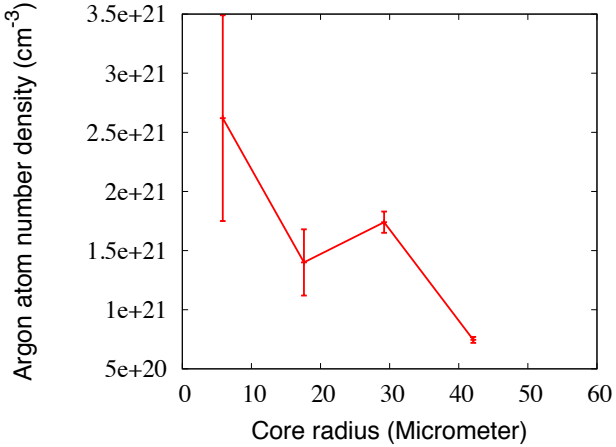

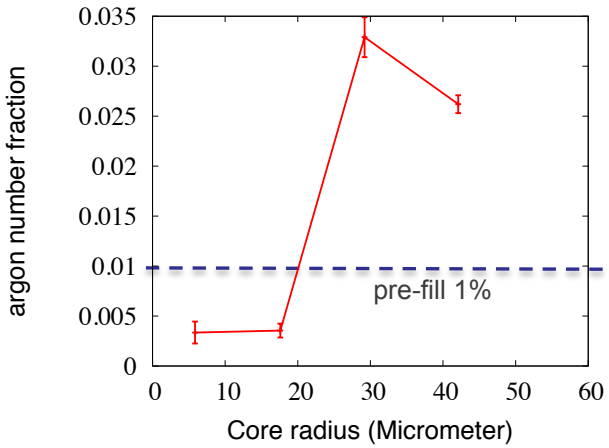

Calculated space-resolved spectra are a better fit to data with species separation effects turned on in the simulations

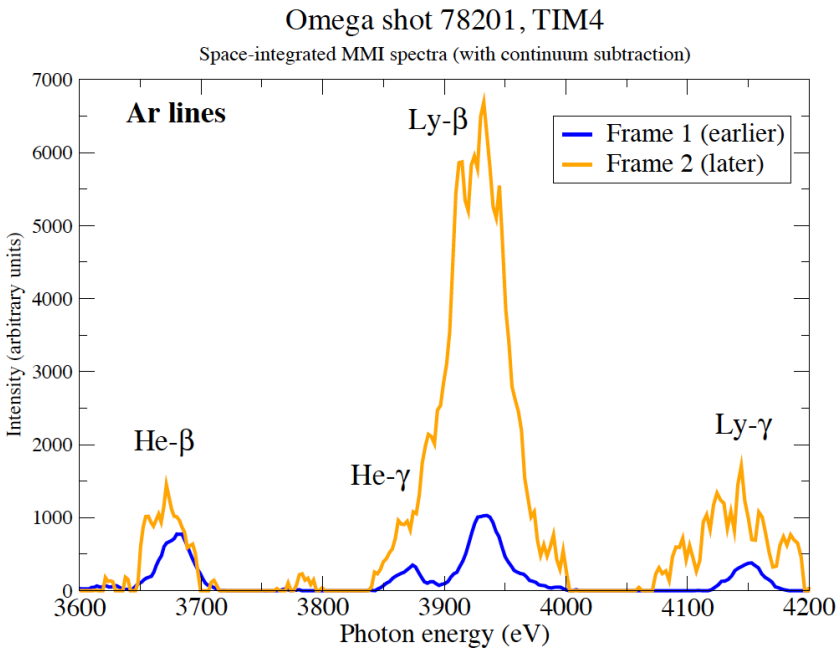

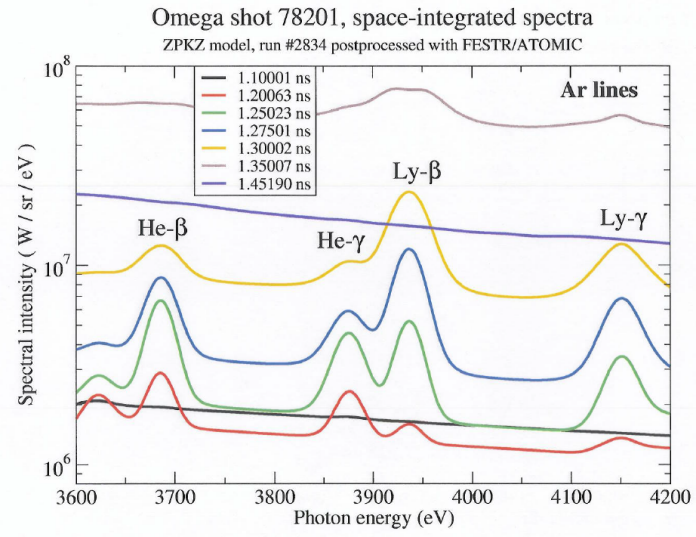

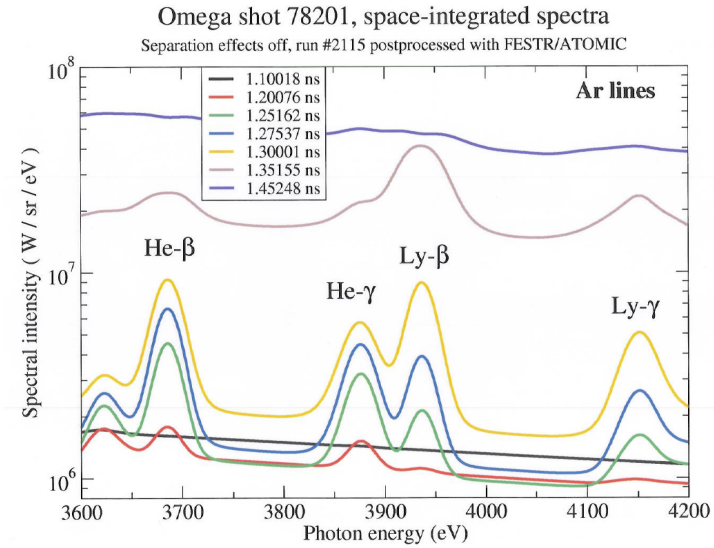

Conclusions

- **We used x-ray spectroscopy to observe interspecies ion separation by exploiting large ion thermo-diffusion between species with large mass difference (D/Ar)**

- **Analyses of MMI data provide Ar-concentration vs. radius at different times, resulting in direct experimental inference of D/Ar separation**
  - **1D spherical symmetry assumed in analysis; however, 2D/3D effects may be important**

- **Simulations using two different multi-ion-species diffusion models (MSV, ZPKZ) aid our data interpretation**
  - **Calculated maximum amounts of Ar enhancement/depletion agree reasonably well with experiment**
  - **Calculated Ar-concentration profile across incoming shock may correspond to experimental observations (more work needed to pin this down)**
  - **Species separation is attributable to ion thermo-diffusion in the simulations**

- **These results encourage us to propose further campaigns on OMEGA to explore the scalings predicted by interspecies-ion-diffusion theory**

Backup slides

Theory provided quantitative design goals

Diffusion coefficient *D* and diffusion ratios *k* are given in closed-form, where *A* and *B* require kinetic calculations:

$$D = \frac{\rho T_i}{A_{lh}\mu_{lh}n_l\nu_{lh}} \times \frac{c(1-c)}{cm_h + (1-c)m_l},$$

$$k_p = c(1-c)(m_h - m_l)\left(\frac{c}{m_l} + \frac{1-c}{m_h}\right),$$

$$k_E = m_l m_h c(1-c)\left(\frac{c}{m_l} + \frac{1-c}{m_h}\right)\left(\frac{Z_l}{m_l} - \frac{Z_h}{m_h}\right),$$

$$k_T^{(i)} = m_l m_h\left(\frac{c}{m_l} + \frac{1-c}{m_h}\right)\left[\frac{cB_{ll}}{m_l} + \frac{(1-c)B_{lh}}{m_h}\right],$$

$$k_T^{(e)} = m_l m_h\left(\frac{c}{m_l} + \frac{1-c}{m_h}\right)\left[\frac{cZ_l}{m_l} + \frac{(1-c)Z_h}{m_h}\right] \times [(1-c)B_{le} - cB_{he}]\frac{T_e}{T_i},$$

G. Kagan and X.-Z. Tang, Phys. Plasmas **19**, 082709 (2012).
G. Kagan and X.-Z. Tang, Phys. Rev. Lett. **109**, 269501 (2012).
G. Kagan and X.-Z. Tang, Phys. Lett. A **378**, 1531 (2014).

$$\tau_{\rm diff} \sim n_{Ar} Z_{Ar}^2 T_i^{-5/2}$$

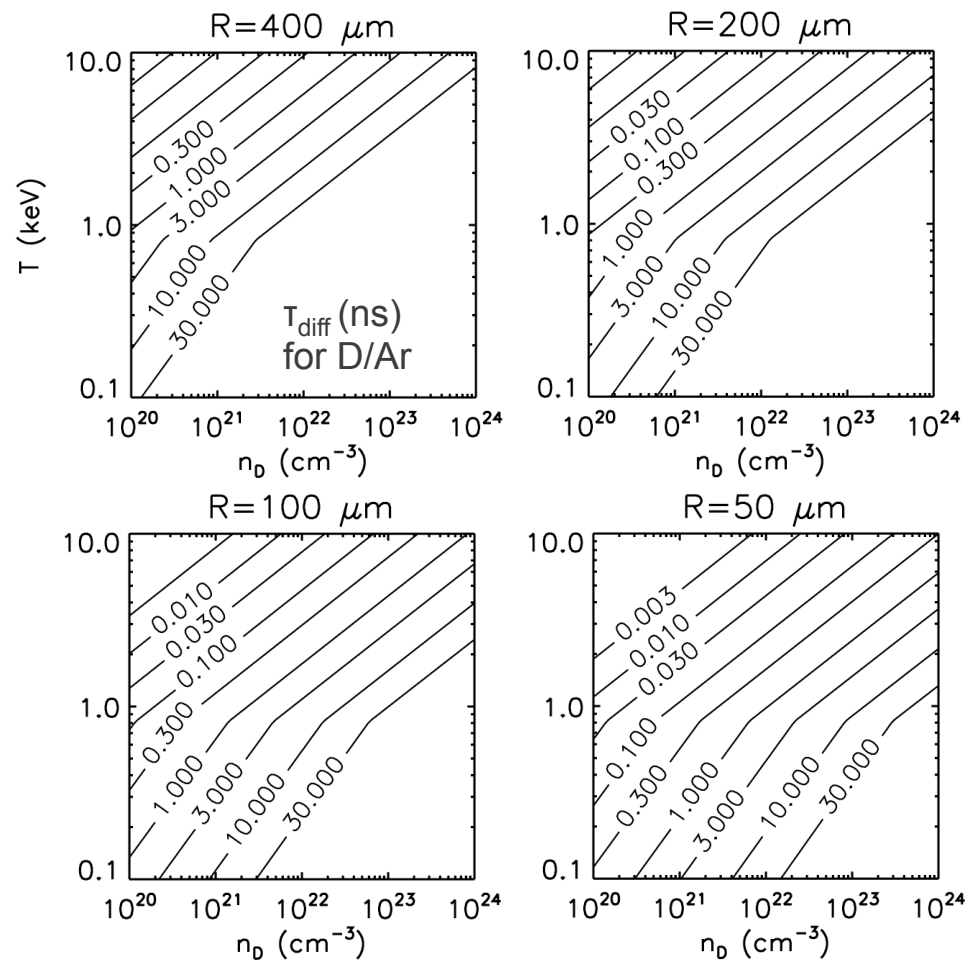

Want high-temperature (T_i>4 keV), low-density (n_D<10^{24} cm^{-3}) implosion!

Diffusion ratios for other binary mixtures

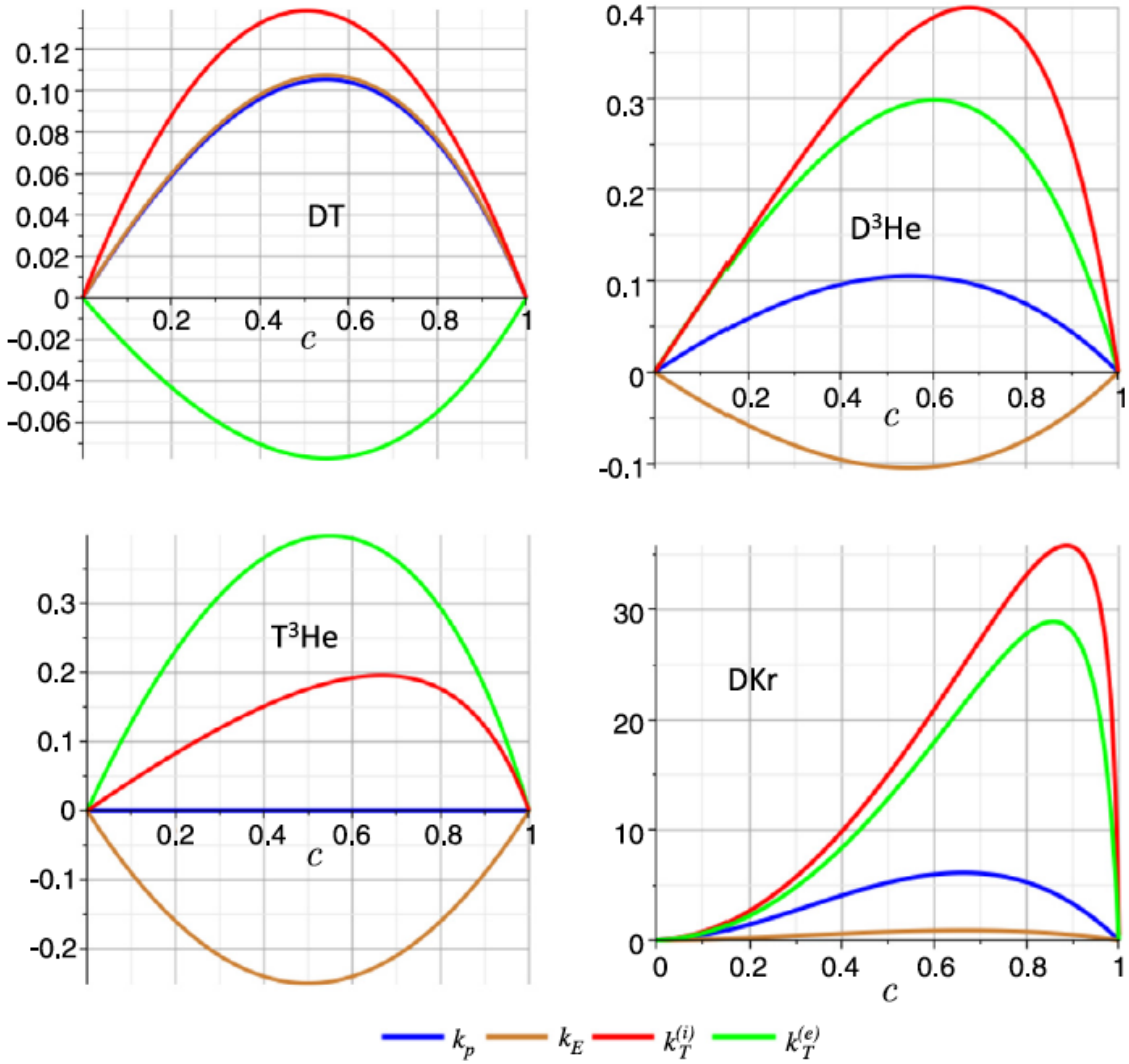

G. Kagan and X.-Z. Tang, Phys. Lett. A **378**, 1531 (2014).

D/Ar collisional mean free paths and Knudsen numbers are small compared to hot-spot size throughout implosion

D/Ar mean free path in μm

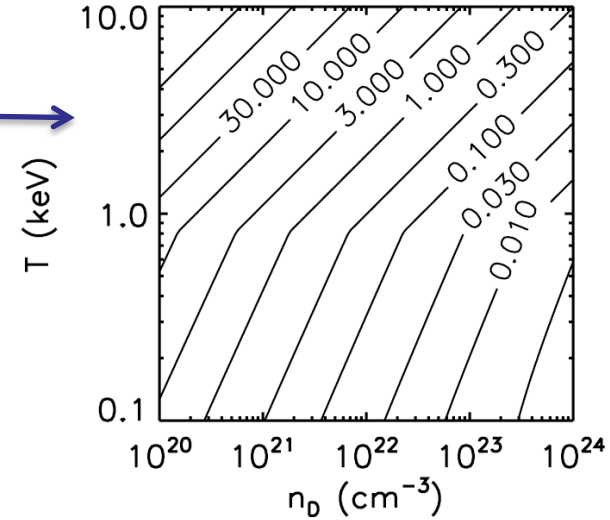

$Kn = \lambda_{D/Ar} / (R/2)$

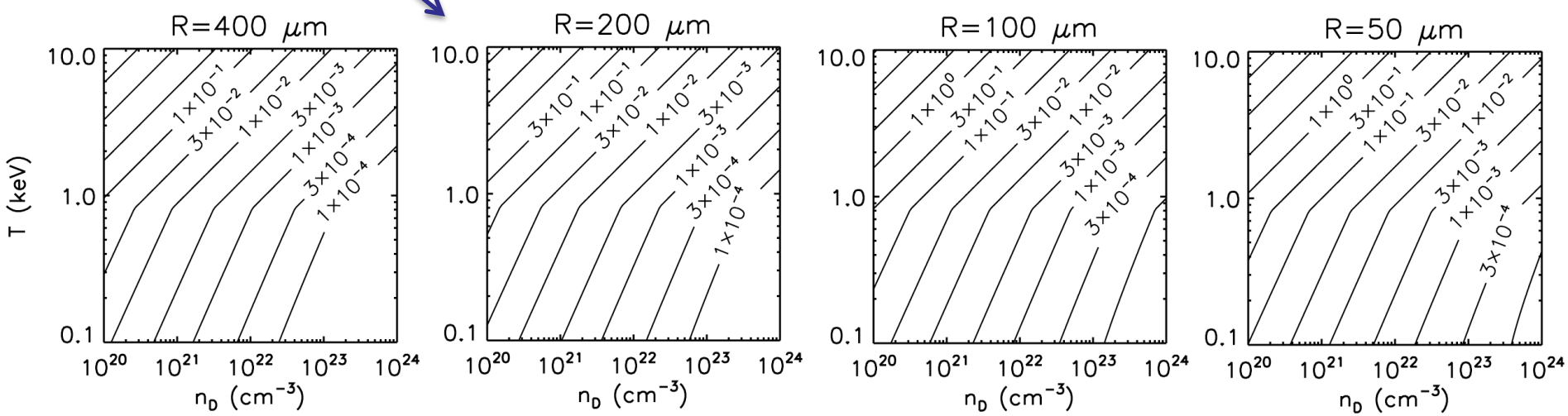

Ar atom% vs. D mass concentration *c*

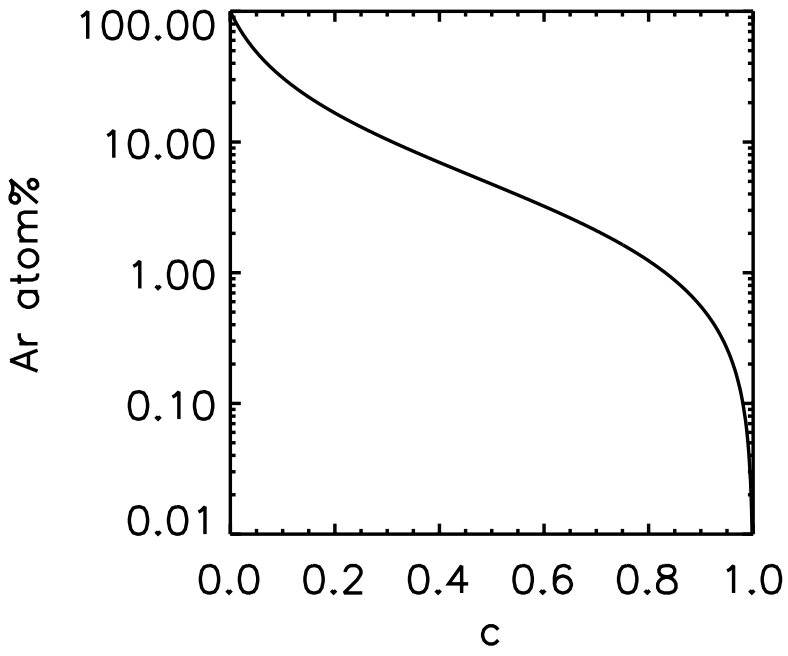

We use two independent analysis methods to infer interspecies D/Ar separation

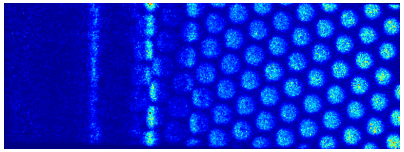

MMI data
(spectrally resolved 2D images)

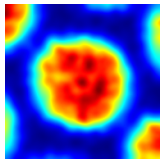

Broadband and narrowband images
(Ar He-β, Ly-β, Ly-γ)

Photocalibrate with
XRS/SSCA data

Spectroscopic analysis w/Abel inversion gives $n_e(R)$, $T_e(R)$, $n_{Ar}(R)$

Extract radially resolved spectra by applying "masks" on broadband images

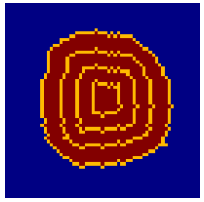

Quasi-neutrality assumption gives n_{Ar} / n_D vs. R

Best fit to FESTR/ATOMIC provides n_e, T_e, and n_{Ar} / n_D vs. R

Based on L. Welser-Sherrill et al., Phys. Rev. E **76**, 056403 (2007).

Radially resolved spectra based on Nagayama et al., Phys. Plasmas **21**, 050702 (2014); FESTR: P. Hakel, Comput. Phys. Comm. (submitted); ATOMIC: Fontes et al., in *Modern Methods in Collisional-Radiative Modeling of Plasmas* (Springer, New York, 2016).

MMI timing is pinpointed by comparing to SSCA and postprocessed hydrodynamic x-ray time history

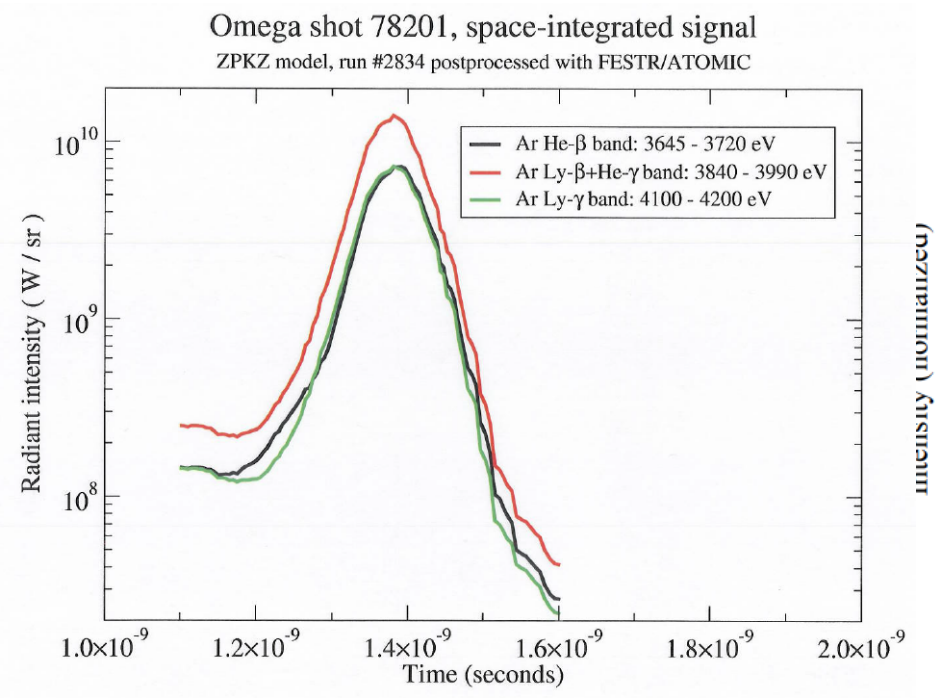

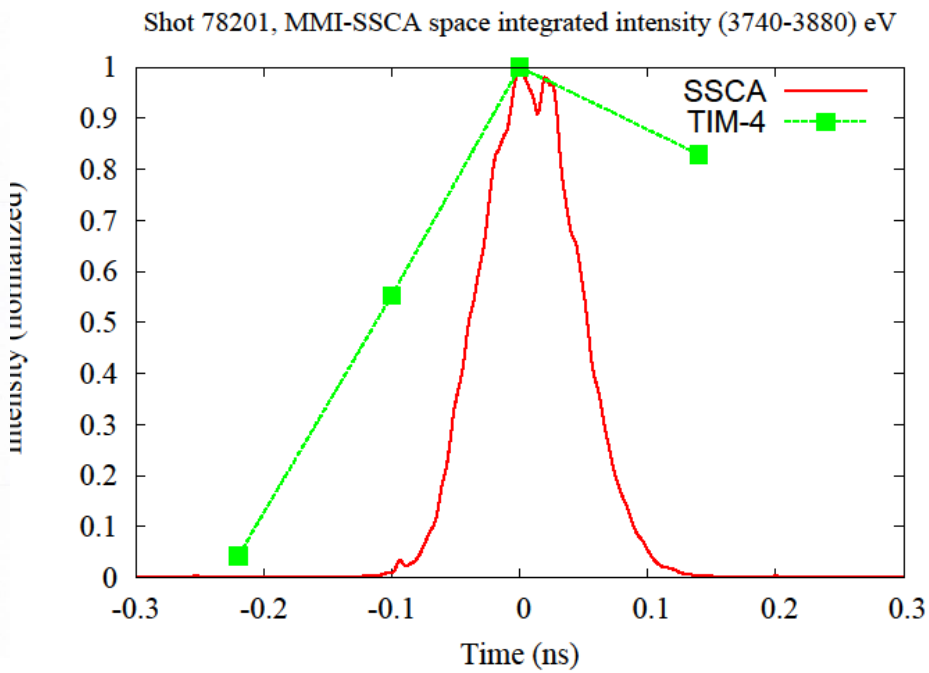

Comparisons suggest that MMI TIM4/F2 occurs ~100 ps before peak in X-ray emission

Shot 78201 additional analysis: (i) peak emission from TIM3 is close to neutron BT; (ii) 1% CH mix throughout fuel does not alter conclusion of D/Ar separation

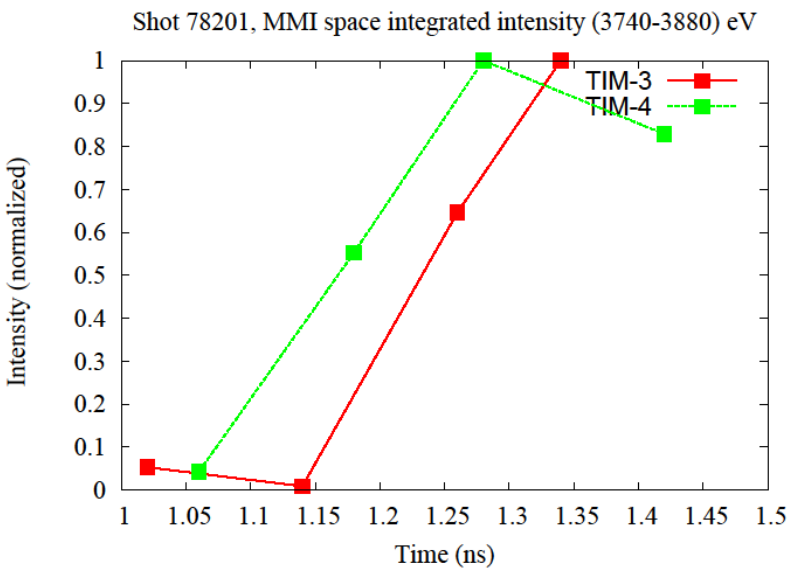

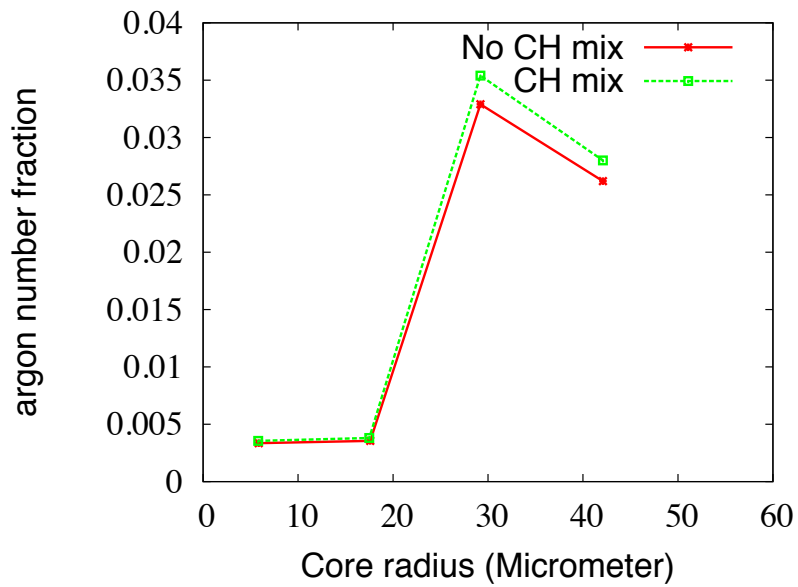

SSCA provides a check on MMI trigger timings provided to us by OMEGA operations team

Shot 78199, XRFC1/TIM3/f2, 13 μm/5 atm/1% Ar
t_{BT}=1.313 ns, DDn=1.35E11, 21.1 kJ UV

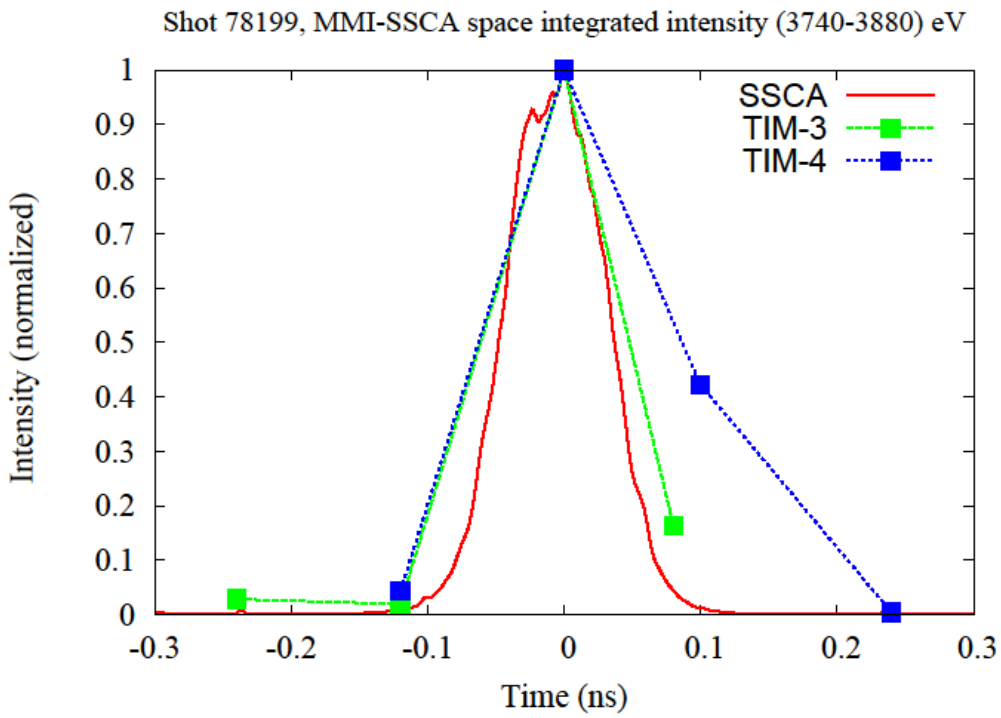

xRAGE simulations including MSV model for interspecies ion transport compare well with MMI-extracted n_e and T_e
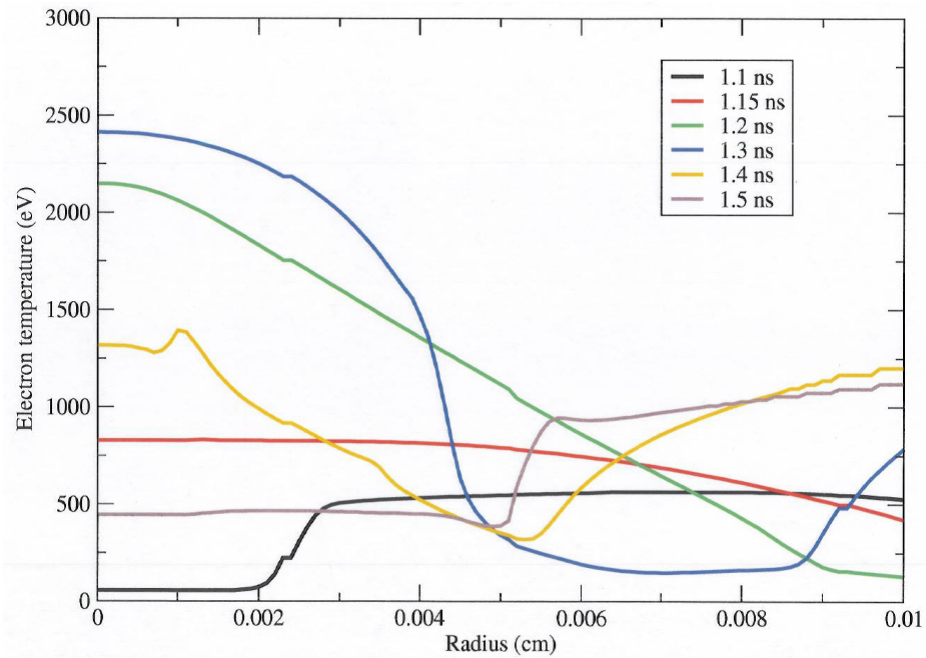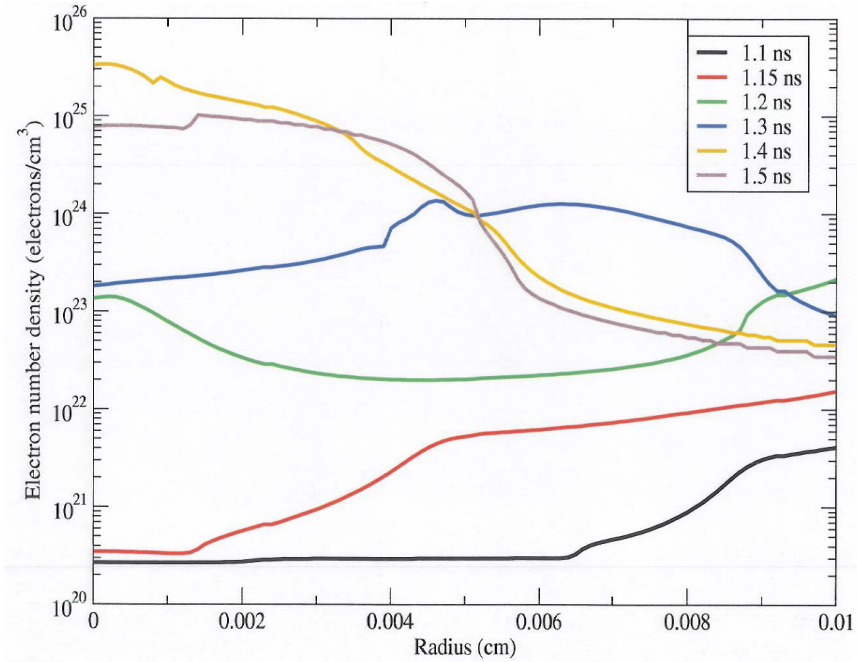
Shot 78199 simulation by E. Vold